# **Dalton** Transactions



**PAPER** 

View Article Online



Cite this: Dalton Trans., 2018, 47,

Received 22nd December 2017, Accepted 28th January 2018 DOI: 10.1039/c7dt04860b

rsc li/dalton

# N,N-Disubstituted-N'-acylthioureas as modular ligands for deposition of transition metal sulfides†

Zahra Ali, ‡<sup>a,b</sup> Nathaniel E. Richey, (10 ‡ Duane C. Bock, (10 a Khalil A. Abboud, a Javeed Akhtar. Muhammad Sherb and Lisa McElwee-White \*\*

First row transition metal complexes (Ni, Co, Cu, Zn) with N,N-disubstituted-N'-acylthiourea ligands have been synthesized and characterized. Bis(N,N-diisopropyl-N'-cinnamoylthiourea)nickel was found to have the lowest onset temperature for thermal decomposition. Thin film deposition of Ni, Co, and Zn sulfides by aerosol assisted chemical vapor deposition from their respective N,N-diisopropyl-N'-cinnamoylthiourea complexes at 350 °C has been demonstrated.

## Introduction

Transition metal sulfides are a promising class of semiconductors that show potential in a wide range of energy and photonic related applications.<sup>1,2</sup> The materials properties of the metal sulfide are important when considering appropriate applications. For example, crystalline materials are typically better for photonic applications,3 while amorphous metal sulfides are promising for their use in lithium ion batteries and as electrocatalysts. 4,5 In attempts to control the properties of the materials, a multitude of strategies have been employed in their synthesis. Among the techniques that have been explored are variants of solvothermal processes and chemical vapor deposition (CVD).6 For these methods, single source precursors (SSP), in which both metal and sulfide source are the same compound, are often able to produce the metal sulfide at lower temperatures and with better control of stoichiometry. Many of these single source precursors lack the volatility to be used in conventional CVD, where volatilization of neat precursor occurs in a bubbler. However, this limitation can be overcome by using aerosol-assisted (AA)CVD, in which the precursor is dissolved in an appropriate solvent and nebulized for transport to the substrate.8,9 Since volatility is not critical for AACVD precursors, the technique allows exploration

of ligand chemistry that could not be used in conventional CVD. Study of new ligands can provide a means to tune the

stoichiometry of the deposited material, increase atmospheric

stability, and control the decomposition temperature of the

Dithiocarbamate ligands have been widely used in deposition of a wide range of metal sulfides, such as iron, copper, cobalt, nickel, zinc, molybdenum, tungsten, and tin. 13-17 These complexes often do not require special handling, however this comes at the price of higher deposition temperatures, typically above 300 °C. Xanthate ligands have similarly found use with a variety of metals and often decompose at lower temperatures than their dithiocarbamate analogues. 18-20 This lowered decomposition temperature of the xanthate precursors comes from the Chugaev elimination mechanism pathway by which these ligands can readily decompose to their corresponding metal sulfide.21 Thiobiuret and dithiobiuret complexes have also found use for the deposition of a wide variety of late transition metal sulfides and show no oxygen incorporation from the thiobiurets.<sup>22,23</sup> Several other ligands, such as thioureas and dithiophosphates, have also been used though less commonly.24,25

N,N-Disubstituted-N'-acylthiourea ligands have long been known to coordinate to many transition metals in a chelating fashion similar to acetylacetonate. 26,27 Thermogravimetric analysis (TGA) of several of these complexes is consistent with thermal decomposition to the corresponding metal sulfide or pure metal.<sup>28,29</sup> However, the complexes are not sufficiently volatile for conventional CVD. There are a few reports of their use in AACVD but these studies do not explore the effects on

precursor.10 Currently, there are several ligands that are commonly used in single source precursors for the AACVD of metal sulfides. Metal thiolates have been used to deposit metal sulfides at temperatures as low as 150 °C, however their reactivity with air and water makes them difficult to work with. 11,12

<sup>&</sup>lt;sup>a</sup>Department of Chemistry, University of Florida, Gainesville, Florida, 32611, USA. E-mail: lmwhite@chem.ufl.edu

 $<sup>^</sup>b$ Department of Chemistry, Allama Iqbal Open University, Islamabad, Pakistan <sup>c</sup>Department of Chemistry, Polymers & Materials Synthesis Lab (PMS), Mirpur University of Science & Technology (MUST), Alama Iqbal Road, Mirpur, Azad Kashmir, Pakistan

<sup>†</sup> Electronic supplementary information (ESI) available: Metal complex TGA and DTG plots, PXRD of the deposits, and X-ray crystallographic data. CCDC 1811086-1811089. For ESI and crystallographic data in CIF or other electronic format see DOI: 10.1039/c7dt04860b

<sup>‡</sup>These authors have contributed equally to this work.

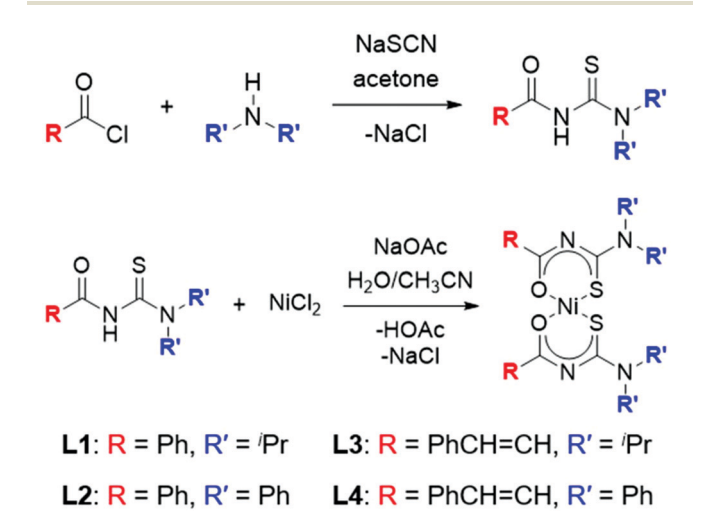
**Paper** 

decomposition temperature from varying the substituents on the ligand. 30,31 Herein, we investigate the impact of the N-substituents, R and R' on decomposition temperatures of Ni complexes and demonstrate that these ligands can be used for deposition of metal sulfides via AACVD.

## Results and discussion

To investigate the effect of substituents, we synthesized and compared four nickel complexes with ligands derived from two acid chlorides, benzoyl and cinnamoyl chloride, and two secondary amines, diphenyl- and diisopropylamine. The N,Ndisubstituted-N'-acylthiourea ligands are readily synthesized in a two-step, one-pot reaction by mixing the acid chloride and sodium thiocyanate, followed by addition of the secondary amine (Scheme 1).32 After purification by recrystallization from an appropriate solvent mixture, the ligand was deprotonated with a mild base and reacted with a metal salt to form the respective ML<sub>2</sub> or ML<sub>3</sub> complex in good yield. <sup>33</sup> The wide range of commercially available acid chlorides and secondary amines make this family of ligands highly modular.

The thermal behavior of these complexes was investigated by both TGA and the first derivative of the TGA plot (DTG) (Fig. 1). From these data, it was observed that Ni(L3)2 (where R = PhCH = CH,  $R' = {}^{i}Pr$ ) has the lowest decomposition temperature, with mass loss occurring most rapidly at 223 °C. An increase of approximately 25 °C in decomposition temperature is observed for Ni(L1)2, in which R is phenyl. A similar increase of approximately 25 °C in the decomposition temperature is observed in comparison of Ni(L4)2 and Ni(L2)2. Varying R' from alkyl to aryl moiety also caused a significant increase in decomposition temperature, with a difference of approximately 45 °C between Ni(L1)2 and Ni(L2)2 as well as between Ni(L3)<sub>2</sub> and Ni(L4)<sub>2</sub>. This resulted in a total difference of 70 °C in the decomposition of Ni(L3)2 and Ni(L2)2, even though the ligand backbone remained unchanged. This shows



Scheme 1 Synthesis of N,N-disubstituted-N'-acylthioureas and nickel complexes.

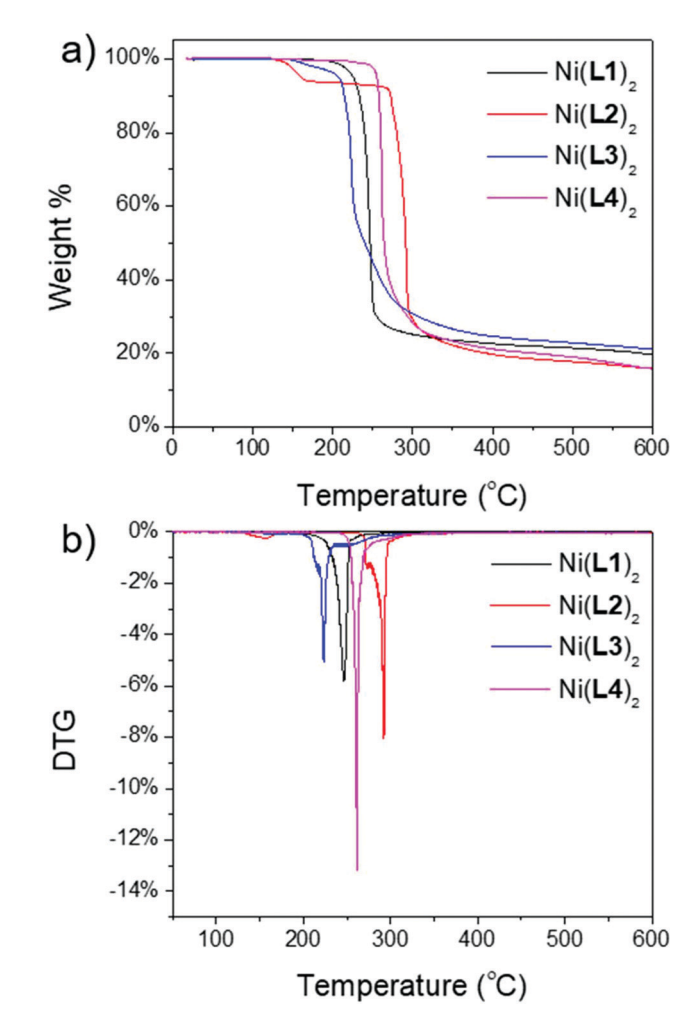


Fig. 1 (a) TGA and (b) DTG plots of the Ni(L1-4)<sub>2</sub> complexes.

that decomposition temperature is directly correlated to the substituents and that both R and R' need to be carefully considered when designing precursors based on this ligand framework.

Fragmentation from mass spectrometry has previously been used as a model for the gas phase decomposition of precursors in CVD, though some care needs to be taken in interpretation.34,35 Tandem mass spectrometry was used to elucidate possible decomposition pathways of Ni(L3)2. In this experiment the [M + H]+ ion was selectively trapped and fragmentation was brought on by collision induced dissociation until the parent peak was no longer visible (Fig. S6, ESI†). A list of abundant ions observed in positive mode appears in Table 1. The base peak is observed at m/z 510.93 and is attributed to loss of diisopropylcyanamide ( $[M + H - N(^{i}Pr)_{2}CN]^{+}$ ). The second largest peak is observed at m/z 507.07 and is attributed to the loss of the cinnamoyl moiety ([M + H - PhCH=CHCO]<sup>+</sup>). In these two most abundant fragments the Ni-S bond is unaffected. This may be indicative of the preference for these complexes to decompose to the metal sulfide. Another fragment is observed for the Ni(L3)(diisopropylcyanamide) complex at m/z 473.17 ([M + H - PhCH=CHCOSH]<sup>+</sup>) with a

**Dalton Transactions** 

Table 1 Selected relative abundance of ion fragments from tandem mass spectrometry of Ni(L3)<sub>2</sub>

m/z	Fragment	Relative abundance	
637.07	$[M + H]^+$	0	
535.87	$[M + H - NH(^{i}Pr)_{2}]^{+}$	44.3	
510.93	$[M + H - N(^{1}Pr)_{2}CN]^{+}$	100	
507.07	$[M + H - PhCH = CHCO]^+$	92.1	
473.17	$[M + H - PhCH = CHCOSH]^+$	91.0	
347.07	$[M + H - HL3]^+$	55.7	

high relative abundance. If this fragment were also formed during the thermal gas phase reaction, the cyanamide would be expected to be labile, similarly to what has been reported for acetonitrile adducts of tungsten imido precursors.<sup>34</sup> This secondary fragmentation (loss of the cyanamide) would

provide another route to the ion observed at m/z 347.07 ([M + H - HL3]<sup>+</sup>), corresponding to overall loss of the L3 ligand. Loss of the HNR'<sub>2</sub> moiety is also observed in good abundance at m/z 535.87 ([M + H - NH( $^{1}$ Pr)<sub>2</sub>]<sup>+</sup>).

Since among all nickel complexes,  $Ni(L3)_2$  had the lowest decomposition temperature, L3 was selected for the synthesis and study of several other  $ML_2$  and  $ML_3$  complexes (M=Ni, Zn, Co, and Cu). The formation of all of the metal complexes could be easily followed with IR spectroscopy during synthesis by observing the disappearance of the amide N-H and C=O stretches of the free ligand. For the diamagnetic complexes, Ni (L1-4)<sub>2</sub>,  $Co(L3)_3$ , and  $Zn(L3)_2$ , the disappearance of the N-H proton in  $^1H$  NMR could also be followed.

The X-ray crystal structures were determined for all  $M(L3)_2$  and  $M(L3)_3$  complexes (Tables 2–4). Ni(L3)<sub>2</sub> showed a square

Table 2 Selected crystal data and structure refinement data

	$Ni(L3)_2$	$Cu(L3)_2 \cdot THF$	$Co(L3)_3$	$Zn(L3)_2 \cdot NCCH_3$
Formula	C <sub>32</sub> H <sub>42</sub> NiN <sub>4</sub> O <sub>2</sub> S <sub>2</sub>	C <sub>36</sub> H <sub>50</sub> CuN <sub>4</sub> O <sub>3</sub> S <sub>2</sub>	C <sub>48</sub> H <sub>63</sub> CoN <sub>6</sub> O <sub>3</sub> S <sub>3</sub>	C <sub>34</sub> H <sub>45</sub> ZnN <sub>3</sub> O <sub>2</sub> S <sub>2</sub>
Crystal system	Tetragonal	Triclinic	Monoclinic	Monoclinic
Space group	$Iar{4}$	$Par{1}$	$P2_{I/c}$	$P2_{I/n}$
$a(\mathring{A})$	14.662(2)	10.5648(7)	9.6733(4)	13.8922(16)
b (Å)	14.662(2)	11.9358(8)	26.7438(10)	7.4030(9)
a (Å) b (Å) c (Å)	15.487(2)	15.2248(10)	18.9117(7)	34.250(4)
$\alpha$ (°)	90	79.6830(10)	90	90
$\beta$ $(\circ)$	90	72.2510(10)	92.5405(9)	99.859(2)
$\gamma$ (°)	90	84.0150(10)	90	90
Volume (ų)	3329.2(11)	1796.4(2)	4887.7(3)	3470.4(7)
$D_{\rm calc}({\rm Mg~m}^{-3})$	1.272	1.173	1.260	1.312
Total reflns	36 001	36 766	114 933	34 093
Unique reflns	5829	8897	18 743	8616
$GOF$ of $F^2$	1.029	1.025	1.016	0.829

 $\textbf{Table 3} \quad \text{Selected bond distances (Å) for Ni(L3)$_2$, Cu(L3)$_2$. THF, Co(L3)$_3$, and Zn(L3)$_2$. NCCH$_3$ and Zn(L3)$_2$. The control of the contro$ 

Compound	Bond	M-O bond lengths	M-S bond lengths	Bond	Backbone C–N lengths
Ni(L3) <sub>3</sub>	Ni1-O1/S1	1.8719(9)	2.1424(4)	C1-N1, C2-N1	1.3283(16), 1.3441(16)
$Cu(L3)_2 \cdot THF^a$	Cu1-O1/S1	1.9093(13)	2.2709(4)	C1-N1, C2-N1	1.323(2), 1.354(2)
$Co(L3)_3$	Co1-O1/S1	1.9080(14)	2.2106(6)	C1-N1, C2-N1	1.335(3), 1.339(3)
` '	Co1-O21/S21	1.9463(13)	2.2243(5)	C21-N21, C22-N21	1.337(2), 1.340(2)
	Co1-O41/S41	1.9255(13)	2.2032(6)	C41-N41, C42-N41	1.329(3), 1.336(4)
$Zn(L3)_2 \cdot NCCH_3$	Zn1-O1/S1	1.968(3)	2.2706(11)	C1-N1, C2-N1	1.324(5), 1.351(5)
	Zn1-O21/S21	1.959(3)	2.3083(12)	C21-N21, C22-N21	1.313(5), 1.359(5)

<sup>&</sup>lt;sup>a</sup> Lengths from the ordered molecule within the unit cell.

Table 4 Selected bond distances (Å) for Ni(L3)<sub>2</sub>, Cu(L3)<sub>2</sub>·THF, Co(L3)<sub>3</sub>, and Zn(L3)<sub>2</sub>·NCCH<sub>3</sub>

Compound	Bonds	S-M-S angles	Bonds	Backbone C-N-C angles	Dihedral intersect	Dihedral angles
$Ni(L3)_2$ $Cu(L3)_2$ ·THF <sup>a</sup> $Co(L3)_3$	S1-Ni1-S2 S1-Ni1-S2 S1-Co1-S42 S1-Co1-S42 S21-Co1-S42 S1-Zn1-S2	83.83(2) 180.0 89.47(2) 86.76(2) 89.31(2) 121.76(4)	C1-N1-C2 C1-N1-C2 C1-N1-C2 C21-N21-C22 C1-N1-C2 C1-N1-C2 C21-N21-C22	124.36(11) 125.10(16) 125.53(17) 123.69(15) 126.3(2) 126.8(3) 126.4(3)	N1 N1 N1 N21 N41 N1 N21	13.536(161) 32.825(221) 8.980(360) 34.806(211) 20.638(373) 42.087 (0.413) 50.317(416)

<sup>&</sup>lt;sup>a</sup> Angles from the ordered molecule within the unit cell.

Fig. 2 X-ray crystallographic structures of (a) Ni(L3)<sub>2</sub> (b) Cu(L3)<sub>2</sub> (c) Co(L3)<sub>3</sub> and (d) Zn(L3)<sub>2</sub>. Selected solvent molecules and disorder omitted for clarity.

planar geometry with the sulfurs cis to one another and a S1-Ni1-S1A bond angle of 83.83(2)° (Fig. 2a). The cis isomer has been noted for other nickel complexes of N,N-disubstituted-N'acylthioureas as well and by analogy, we assign the predominant isomer for Ni(L1)<sub>2</sub>, Ni(L2)<sub>2</sub>, and Ni(L4)<sub>2</sub> as cis.<sup>30</sup> The Cu(L3)<sub>2</sub> crystal structure contained two copper centers, one ordered and the other disordered, and two disordered tetrahydrofuran molecules from the crystallization process resulting in an overall formula of Cu(L3)2·THF (Fig. S2, ESI†). Cu(L3)2·THF also showed square planar geometry, however the coordination around copper was trans with respect to the sulfurs with a S1-Cu1-S1A angle of 180.0° (Fig. 2b). The difference in cis and trans coordination around nickel and copper, respectively, has been observed previously for similar bis(thiobiuret) complexes.<sup>22</sup> The cobalt(II) ion in the starting material CoCl2 was oxidized during the synthesis of Co(L3)<sub>3</sub>, consistent with the diamagnetic <sup>1</sup>H NMR spectrum. The crystal structure shows Co(L3)<sub>3</sub> as the facial isomer with S-Co-S angles ranging from 86.31(2) to 89.47(2)° (Fig. 2c). Zn(L3)<sub>2</sub> crystallized in a distorted tetrahedral geometry indicated by the S1-Zn-S2 angle of 120.76(4)° (Fig. 2d). A noninteracting acetonitrile molecule was also present in the asymmetric unit from the crystallization process (Fig. S4, ESI†).

While the coordination around the metal center varies significantly among these complexes, several common characteristics are observed. As expected, the metal-sulfide bonds were significantly longer, approximately 0.3 Å on average, than the metal-oxide bonds due to the increased ionic radius of the sulfur. The bond lengths between the core nitrogen (N1, N21, or N41) and the neighboring carbons (C1/C2, C21/C22, or C41/ C42) do not differ significantly, indicating resonance delocalization through the ligand core. The ligand backbone was distorted from the planarity expected for the free ligand. The dihedral angle between the OCN and SCN planes (Fig. S5, ESI†), where N is the core nitrogen of the backbone (N1, N21, or N41) is less pronounced in  $Ni(L3)_2$  and one of the ligands in  $Co(L3)_3$ with angles of 13.536(161) and 8.980(360)°, respectively, but was larger in Zn(L3)2·NCCH3 with angles of 42.087(0.413) and 50.317(416)°. This dihedral angle also varied significantly for ligands on the same metal center and range between 8.980(360), 34.806(211), and 20.638(373)° on the Co(L3)<sub>3</sub> complex. These

**Dalton Transactions** Paper

factors also cause the C-N-C angle in the ligand to open up to values from 123.69(15) to 126.8(3)° (Tables 3 and 4).

TGA and DTG of the Cu(L3)2·THF, Co(L3)3, and Zn(L3)3 complexes showed similar decomposition temperatures to that of Ni(L3)2 (Fig. S7, ESI†). From the DTG trace, both Co(L3)3 and Cu(L3)<sub>2</sub> appear to undergo a multistep decomposition pathway. With these relatively low decomposition temperatures, these compounds were precursor candidates for the AACVD of their corresponding metal sulfide. Toluene solutions of 0.65 mM were prepared for the Ni(L3)2, Co(L3)3, and Zn(L3)2 complexes and depositions onto silicon substrates were carried out at 350 °C. Cu(L3)<sub>2</sub> was inadequately soluble in toluene for these depositions and attempts to deposit Cu(L3)2 from a tetrahydrofuran solution at 350 °C were unsuccessful, as indicated by absence of the metal sulfide on the substrate by EDX or PXRD.

Deposition from Ni(L3)2 resulted in a mixture of individual nanorods and thin sheets, which appeared to be fused from several nanorods (Fig. 3a). Growth from Co(L3)3 resulted in the deposition of platelets perpendicular to the substrate with an underlying thin film (Fig. 3b). Zn(L3)<sub>2</sub> appeared to give the most conformal film, with minimal surface features (Fig. 3c). EDX of these depositions resulted in an M:S ratio ranging from 1.0:0.84-1.06 (Table 5). This is within the error for the metal monosulfide deposition, however this is also within range of the sulfur deficient Ni<sub>9</sub>S<sub>8</sub> and Co<sub>9</sub>S<sub>8</sub> phases, which are also known. PXRD revealed mostly amorphous deposits, with only ZnS showing some crystallinity by the presence of a small peak at 28.5° which is indicative of the ZnS (111) reflection (Fig. S8, ESI†). Several peaks from the silicon substrate were also observed in the NiS and ZnS deposits. No increase in crystallinity was observed after annealing at 650 °C for one hour.

## Conclusions

In summary, we have demonstrated that the thermal decomposition temperatures of bis(N,N-disubstituted-N'-acylthiourea) nickel complexes vary with the substituents R and R'. Ni(L3)2 (where R is PhCH=CH and R' is isopropyl) had the lowest decomposition temperature, with the most rapid mass loss occurring at 223 °C. The related complexes Ni(L3)<sub>2</sub>, Cu(L3)<sub>2</sub>, Co(L3)<sub>3</sub>, and Zn(L3)<sub>2</sub> were all synthesized and found to crystalize in the cis-square planar, trans-square planar, fac-octahedral, and distorted tetrahedral geometries respectively. Ni(L3)<sub>2</sub>, Co(L3)<sub>3</sub>, and Zn(L3)<sub>2</sub> were found to deposit their corresponding metal sulfide from AACVD at temperatures of 350 °C but attempted depositions from tetrahydrofuran solution of Cu(L3)2 were unsuccessful due its low solubility. These experiments demonstrate the viability of N,N-disubstituted-N'-acylthiourea ligands as sulfur sources in the AACVD of metal sulfides.

## Experimental

#### General information

Reagents were purchased from Sigma Aldrich or Fisher Scientific; DMSO- $d_6$  was purchased from Cambridge Isotopes.

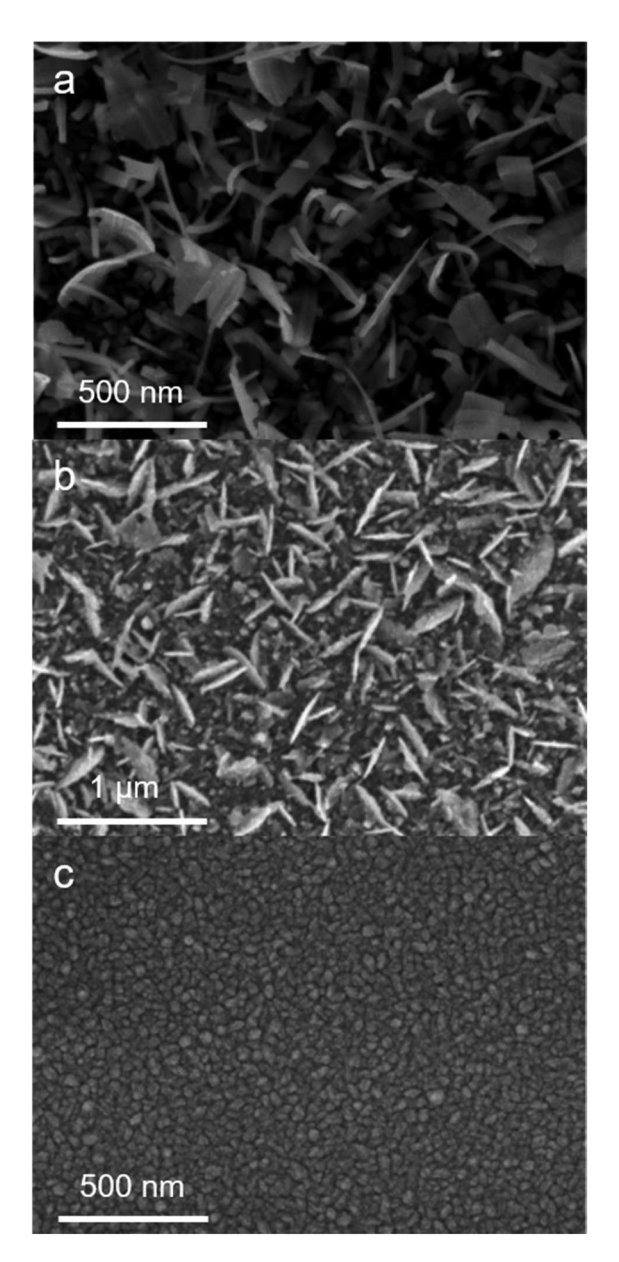


Fig. 3 SEM images of the deposits grown at 350 °C from (a) Ni(L3)<sub>2</sub>, (b)  $Co(L3)_3$ , and (c)  $Zn(L3)_2$ .

Table 5 Metal: sulfur ratios of the deposits

Precursor	M:S ratio	
Ni(L3) <sub>2</sub> Co(L3) <sub>3</sub> Zn(L3) <sub>2</sub>	1:0.90 1.0:0.84 1.0:1.06	

Nitrogen gas (99.999%) was purchased from AirGas. Toluene was purified using an MBraun MB-SP solvent purification system and stored over activated 3 Å molecular sieves for at least 48 h prior to experiments. Acetone was distilled over CaSO<sub>4</sub> and KMnO<sub>4</sub> prior to use. All other reagents were used as received. NMR spectra were recorded on a Varian Mercury

**Paper Dalton Transactions** 

300 (300 MHz) spectrometer using residual protons from deuterated solvents for reference. IR spectra were obtained on a Bruker Vertex 80 V equipped with an ATR diamond crystal stage. Thermogravimetric analysis (TGA, TA Discovery5500) was performed under N2 gas with a heating rate of 10 °C per minute. Mass spectrometry was performed on an Agilent 6220 ESI-TOF with Agilent 1100 LC with electrospray ionization (ESI) or direct analysis in real time (DART) ionization. Elemental CHN analysis was performed by Robertson Microlit laboratories, New Jersey. X-Ray intensity data were collected at 100 K on a Bruker DUO diffractometer using MoKα radiation (l = 0.71073 Å) and an APEXII CCD area detector.

Depositions were carried out using a Blue Wave Semiconductors CVD reactor with a Liquifog ultrasonic liquids atomizer from Johnson Matthey Piezoproducts. The crystallinities and morphologies were measured by X-ray diffraction (XRD, Panalytical X'pert Pro) and field emission scanning electron microscopy (FESEM, FEI Nova NanoSEM 430). Elemental compositions of the deposits were determined by energy-dispersive X-ray spectroscopy (FESEM, FEI Nova NanoSEM 430).

#### Ligand synthesis

General procedure for ligands L1, L2, L3 and L4. This procedure was adapted from a previously reported synthesis. 36,37 The acyl chloride (34 mmol) was stirred with NaSCN (34 mmol) in dry acetone (25 mL) for 10 minutes, after which the solution was milky white. The dialkyl or diaryl amine (34 mmol) was dissolved in dry acetone (15 mL) and was then added to the stirring solution, which turned yellow. The solution was then added to 250 mL of ice cold water, at which point the crude product precipitated. The crude product was filtered, dried, and recrystallized from an acetonitrile: water (3:1) mixture.

L1. Benzoyl chloride (3.95 mL) and diisopropylamine (4.80 mL) were used as the acyl chloride and diamine, respectively. While previously prepared, no spectroscopic data were reported.<sup>37</sup> Yield: 7.0116 g, 78%. <sup>1</sup>H NMR (300 MHz; DMSO-d<sub>6</sub>):  $\delta$  = 10.32 ppm (s, 1H), 7.70 (m, 5H), 4.56 (broad, 1H), 4.30 (s, 1H), 1.36 (d, 12H). FTIR (neat): 3245 cm<sup>-1</sup> (m), 1786 cm<sup>-1</sup> (m), 1650 cm<sup>-1</sup> (s), 1599 cm<sup>-1</sup> (m), 1581 cm<sup>-1</sup> (m), 1538 cm<sup>-1</sup> (m).

L2. Benzoyl chloride (3.95 mL) and diphenylamine (4.80 mL) were used as the acyl chloride and diamine, respectively. The compound was characterized by comparison to literature data.<sup>38</sup> Yield: 10.7371 g, 95%. <sup>1</sup>H NMR (300 MHz; DMSO- $d_6$ ):  $\delta$  = 11.18 ppm (s, 1H), 7.40 (m, 15H). FTIR (neat): 3210 cm<sup>-1</sup> (m), 1690 cm<sup>-1</sup> (s), 1591 cm<sup>-1</sup> (m), 1501 cm<sup>-1</sup> (s).

L3. Cinnamoyl chloride (5.6644 g) and diisopropylamine (4.80 mL) were used as the acyl chloride and diamine, respectively. Yield: 8.0972 g, 82%. <sup>1</sup>H NMR (300 MHz; DMSO- $d_6$ ):  $\delta =$ 10.13 ppm (s, 1H), 7.54 (m, 6H), 6.80 (d, 1H), 4.33 (broad, 1H), 1.39 (broad, 12H). FTIR (neat): 3237 cm<sup>-1</sup> (m), 1661 cm<sup>-1</sup> (m), 1626 cm<sup>-1</sup> (s), 1577 cm<sup>-1</sup> (w), 1526 cm<sup>-1</sup> (s).

L4. Cinnamoyl chloride (5.6644 g) and diphenylamine (4.80 mL) were used as the acyl chloride and diamine, respectively. Yield: 10.6032 g, 87%.  $^{1}$ H NMR (300 MHz; DMSO- $d_6$ ):  $\delta =$ 11.02 ppm (s, 1H), 7.32 (m, 16H), 6.67 (d, 1H). FTIR (neat): 3178 cm<sup>-1</sup> (m), 1704 cm<sup>-1</sup> (s), 1684 cm<sup>-1</sup> (w, sh), 1667 cm<sup>-1</sup> (s), 1634 cm<sup>-1</sup> (s), 1617 cm<sup>-1</sup> (s), 1589 cm<sup>-1</sup> (m), 1535 cm<sup>-1</sup> (m).

## Metal complex synthesis

General procedure for nickel complexes. This procedure was adapted from a previously reported synthesis.<sup>39</sup> Nickel chloride hexahydrate (0.5940 g, 2.5 mmol) was dissolved in (10 mL) of water and was added to a stirring solution of L1-4 (5 mmol) in acetonitrile (35 mL). Sodium acetate (0.8200 g, 10 mmol) in water (10 mL) was then added, resulting in complex precipitation that was filtered off and dried in vacuo.

Ni(L1)<sub>2</sub>. From 1.3220 g of L1, yield: 1.0245 g, 70%. The compound was characterized by comparison to literature data.<sup>39</sup> <sup>1</sup>H-NMR (300 MHz; DMSO- $d_6$ ):  $\delta = 8.18$  (m, 4H), 7.61 (m, 6H), 4.85 (s, 2H), 4.10 (s, 2H), 1.55 (d, 12H), 1.34 (broad, 12H). FTIR (neat): 1587 cm<sup>-1</sup> (w) 1509 cm<sup>-1</sup> (m). MS (ESI) m/z 585.18 (M + H<sup>+</sup>). Elemental analysis: Calc. for C<sub>28</sub>H<sub>38</sub>N<sub>4</sub>O<sub>2</sub>S<sub>2</sub>Ni: C, 57.44; H, 6.54; N, 9.57; found: C, 57.51; H, 6.60; N, 9.57%.

Ni(L2)2. From 1.6621 g of L2, yield: 1.1183 g, 62%. The compound was characterized by comparison to literature data.<sup>39</sup> <sup>1</sup>H-NMR (300 MHz; DMSO- $d_6$ ):  $\delta = 9.00$  (m, 4H), 7.46 (m, 22H), 7.12 (m, 4H). FTIR (neat): 1588 cm<sup>-1</sup> (w), 1508 cm<sup>-1</sup> (s). MS (DART) m/z 721.12 (M + H<sup>+</sup>). Elemental analysis: Calc. for C<sub>40</sub>H<sub>30</sub>N<sub>4</sub>O<sub>2</sub>S<sub>2</sub>Ni: C, 66.59; H, 4.19; N, 7.77. Found: C, 67.04; H, 3.84; N, 7.58%.

Ni(L3)<sub>2</sub>. From 1.4522 g of L3, yield: 1.1165 g, 73%. X-ray quality crystals were obtained from recrystallization in acetonitrile.  ${}^{1}$ H-NMR (300 MHz; DMSO- $d_{6}$ ):  $\delta$  7.63 (m, 6H), 7.42 (m, 6H), 7.00 (d, 2H), 4.85 (s, 2H), 3.95 (s, 2H), 1.49 (broad, 12H), 1.26 (broad, 12H). FTIR (neat): 1638 cm<sup>-1</sup> (m), 1577 cm<sup>-1</sup> (w), 1506 cm<sup>-1</sup> (m). MS (ESI) m/z 637.21 (M + H<sup>+</sup>). Elemental analysis: Calc. for C<sub>32</sub>H<sub>42</sub>N<sub>4</sub>O<sub>2</sub>S<sub>2</sub>Ni: C, 60.29; H, 6.64; N, 8.79. Found: C, 60.29; H, 6.41; N, 8.72%.

Ni(L4)<sub>2</sub>. From 1.7923 g of L4, yield: 1.2377 g, 64%. H-NMR (300 MHz; DMSO- $d_6$ ):  $\delta = 7.49$  (m, 28H), 7.11 (m, 4H), 6.89 (m, 2H). FTIR (neat): 1629 cm<sup>-1</sup> (m), 1589 cm<sup>-1</sup> (w), 1576 cm<sup>-1</sup> (w), 1501 cm<sup>-1</sup> (s). MS (ESI) m/z 773.15 (M + H<sup>+</sup>). Elemental analysis: Calc. for C<sub>44</sub>H<sub>34</sub>N<sub>4</sub>O<sub>2</sub>S<sub>2</sub>Ni: C, 68.32; H, 4.43; N, 7.24. Found: C, 68.22; H, 4.18; N, 7.14%.

Cu(L3)2·THF. Same procedure as for Ni(L3)2, substituting the nickel chloride with cupric nitrate trihydrate (0.6040 g, 2.5 mmol) and recrystallized from THF. Yield: 1.4111 g, 79%. FTIR (neat): 1636 cm<sup>-1</sup> (m), 1577 cm<sup>-1</sup> (w), 1501 cm<sup>-1</sup> (m, sh). MS (ESI) m/z 642.21 ([M - THF + H]<sup>+</sup>). Elemental analysis: Calc. for C<sub>36</sub>H<sub>50</sub>N<sub>4</sub>O<sub>3</sub>S<sub>2</sub>Cu: C 60.52; H, 7.05; N, 7.84. Found: C, 60.41; H, 7.09; N, 7.78%.

Co(L3)<sub>3</sub>. Same procedure for Ni(L3)<sub>2</sub>, substituting the nickel chloride with cobalt chloride hexahydrate (0.5948 g, 2.5 mmol) and 3 equivalents of L3 (7.5 mmol, 2.1782 g). Yield: 1.738 g, 75%. <sup>1</sup>H-NMR (300 MHz; DMSO- $d_6$ ):  $\delta = 7.45$  (m, 18H), 6.80 (d, 3H), 5.40 (broad, 3H), 1.33 (broad, 36H). FTIR (neat): 1633 cm<sup>-1</sup> (m), 1575 cm<sup>-1</sup> (w), 1501 cm<sup>-1</sup> (m). MS (ESI) m/z 927.35 (M + H<sup>+</sup>). Elemental analysis: Calc. for C<sub>48</sub>H<sub>63</sub>N<sub>6</sub>O<sub>3</sub>S<sub>3</sub>Co: C, 62.18; H, 6.85; N, 9.06. Found: C, 62.03; H, 6.44; N, 8.87%.

**Zn(L3)**<sub>2</sub>. Same procedure for Ni(L3)<sub>2</sub>, substituting the nickel chloride with zinc nitrate hexahydrate (0.7437 g, 2.5 mmol). Yield: 1.4495 g, 90%. <sup>1</sup>H-NMR (300 MHz; DMSO- $d_6$ ):  $\delta$  = 7.61 (m, 4H), 7.52 (d, 2H), 7.38 (m, 6H), 6.64 (d, 2H), 5.48 (s, 2H), 3.85 (s, 2H), 1.45 (m, 12H), 1.23 (m, 12H). FTIR (neat): 1636 cm<sup>-1</sup> (m), 1575 (w), 1511 (m, sh). MS (ESI) m/z 643.21 (M + H<sup>+</sup>). Elemental analysis: Calc. for C<sub>32</sub>H<sub>42</sub>N<sub>4</sub>O<sub>2</sub>S<sub>2</sub>Zn: C, 59.66; H, 6.57; N, 8.70. Found: C, 59.76; H, 6.36; N, 9.16%.

#### **Deposition procedure**

Silicon with native silicon dioxide (Si/SiO<sub>2</sub>, n-type, <100>) was cut into squares of approximately 1 cm<sup>2</sup> and cleaned in boiling isopropanol, acetone, and methanol for three minutes each. The substrates were then placed onto the heating stand, placed under vacuum (200-300 mTorr), and heated to 350 °C. In a glovebox, a 0.65 mM solution of precursor was prepared in 20 mL toluene (THF for Cu(L3)<sub>2</sub>) and added to a glass trap. The trap was then removed from the glovebox and connected to the N<sub>2</sub> inlet of the reactor, N<sub>2</sub> was flowed through the trap for 10 min before connecting to the transfer line. The pressure of the reaction chamber was increased to 350 Torr. The trap was then opened to the reaction chamber and nebulization of the solution was started. During the deposition, N2 flow was maintained at 200 sccm and the pressure was maintained at 350 Torr. Once all of the solution had been nebulized (~75 min), the pressure of the reaction chamber was increased to atmospheric pressure and the substrates were cooled to room temperature.

## Conflicts of interest

There are no conflicts to declare.

## Acknowledgements

ZA acknowledges Higher Education Commission (HEC), Pakistan for financial assistance. KAA wishes to acknowledge the National Science Foundation and the University of Florida for funding of the purchase of the X-ray equipment. We thank the UF Mass Spectrometry Research and Education Center, supported by NIH S10 OD021758-01A1, for mass spectrometry data.

### Notes and references

- 1 M.-R. Gao, Y.-F. Xu, J. Jiang and S.-H. Yu, *Chem. Soc. Rev.*, 2013, 42, 2986–3017.
- N. P. Dasgupta, X. Meng, J. W. Elam and A. B. F. Martinson, Acc. Chem. Res., 2015, 48, 341–348.
- 3 P. O'Brien and R. Nomura, *J. Mater. Chem.*, 1995, 5, 1761–1773.
- 4 D. Merki, S. Fierro, H. Vrubel and X. Hu, *Chem. Sci.*, 2011, 2, 1262–1267.
- 5 R. Jin, Q. Zhai and Q. Wang, Chem. Eur. J., 2017, 23, 14056-14063.

- 6 A. N. Gleizes, Chem. Vap. Deposition, 2000, 6, 155-173.
- 7 M. A. Malik, M. Afzaal and P. O'Brien, Chem. Rev., 2010, 110, 4417–4446.
- 8 P. Marchand, I. A. Hassan, I. P. Parkin and C. J. Carmalt, Dalton Trans., 2013, 42, 9406–9422.
- 9 X. Hou and K. L. Choy, *Chem. Vap. Deposition*, 2006, 12, 583–596.
- 10 L. McElwee-White, Dalton Trans., 2006, 5327-5333.
- 11 C. J. Carmalt, S. A. O'Neill, I. P. Parkin and E. S. Peters, J. Mater. Chem., 2004, 14, 830–834.
- 12 S. Schneider, Y. Yang and T. J. Marks, *Chem. Mater.*, 2005, 17, 4286–4288.
- 13 N. E. Richey, C. Haines, J. L. Tami and L. McElwee-White, *Chem. Commun.*, 2017, 53, 7728–7731.
- 14 S. Mlowe, D. J. Lewis, M. A. Malik, J. Raftery, E. B. Mubofu, P. O'Brien and N. Revaprasadu, *Dalton Trans.*, 2016, 45, 2647–2655.
- 15 S. Khalid, M. A. Malik, D. J. Lewis, P. Kevin, E. Ahmed, Y. Khan and P. O'Brien, *J. Mater. Chem. C*, 2015, 3, 12068–12076.
- 16 P. Kevin, D. J. Lewis, J. Raftery, M. Azad Malik and P. O'Brien, J. Cryst. Growth, 2015, 415, 93–99.
- 17 N. Al-Dulaimi, E. A. Lewis, N. Savjani, P. D. McNaughter, S. J. Haigh, M. A. Malik, D. J. Lewis and P. O'Brien, J. Mater. Chem. C, 2017, 5, 9044–9052.
- 18 M. A. Buckingham, A. L. Catherall, M. S. Hill, A. L. Johnson and J. D. Parish, *Cryst. Growth Des.*, 2017, 17, 907–912.
- 19 M. Akhtar, N. Revaprasadu, M. A. Malik and J. Raftery, *Mater. Sci. Semicond. Process.*, 2015, **30**, 368–375.
- 20 N. Alam, M. S. Hill, G. Kociok-Kohn, M. Zeller, M. Mazhar and K. C. Molloy, *Chem. Mater.*, 2008, 20, 6157–6162.
- 21 E. R. T. Tiekink and I. Haiduc, in *Prog. Inorg. Chem*, John Wiley & Sons, Inc., 2005, pp. 127–319.
- 22 K. Ramasamy, M. A. Malik, P. O'Brien and J. Raftery, *Dalton Trans.*, 2010, 39, 1460–1463.
- 23 K. Ramasamy, M. A. Malik, M. Helliwell, J. Raftery and P. O'Brien, *Chem. Mater.*, 2011, **23**, 1471–1481.
- 24 L. P. Mgabi, B. S. Dladla, M. A. Malik, S. S. Garje, J. Akhtar and N. Revaprasadu, *Thin Solid Films*, 2014, **564**, 51–57.
- 25 J. B. Biswal, S. S. Garje, J. Nuwad and C. G. S. Pillai, *J. Solid State Chem.*, 2013, **204**, 348–355.
- 26 N. H. Huy and U. Abram, Inorg. Chem., 2007, 46, 5310-5319.
- 27 N. Selvakumaran, S. W. Ng, E. R. T. Tiekink and R. Karvembu, *Inorg. Chim. Acta*, 2011, **376**, 278–284.
- 28 F. M. Emen and N. Kuelcue, J. Therm. Anal. Calorim., 2012, 109, 1321–1331.
- 29 N. Ozpozan, H. Arslan, T. Ozpozan, M. Merdivan and N. Kulcu, *J. Therm. Anal. Calorim.*, 2000, **61**, 955–965.
- 30 S. Saeed, K. S. Ahmed, N. Rashid, M. A. Malik, P. O'Brien, M. Akhtar, R. Hussain and W.-T. Wong, *Polyhedron*, 2015, 85, 267–274.
- 31 S. Saeed, N. Rashid and R. Hussain, *Eur. Chem. Bull.*, 2013, 2, 409–413.
- 32 A. R. Katritzky, N. Kirichenko, B. V. Rogovoy, J. Kister and H. Tao, *Synthesis*, 2004, 1799.
- 33 A. Mohamadou, I. Dechamps-Olivier and J.-P. Barbier, *Polyhedron*, 1994, 13, 1363–1370.

Paper

34 Y. S. Won, Y. S. Kim, T. J. Anderson, L. L. Reitfort, I. Ghiviriga and L. McElwee-White, *J. Am. Chem. Soc.*, 2006, 128, 13781–13788.

- 35 Y. S. Won, Y. S. Kim, T. J. Anderson and L. McElwee-White, *Chem. Mater.*, 2008, **20**, 7246–7251.
- 36 I. B. Douglass and F. B. Dains, *J. Am. Chem. Soc.*, 1934, **56**, 719–721.
- 37 H. Hartmann, L. Beyer and E. Hoyer, *J. Prakt. Chem.*, 1978, 320, 647–650.
- 38 N. Gunasekaran, P. Ramesh, M. N. G. Ponnuswamy and R. Karvembu, *Dalton Trans.*, 2011, **40**, 12519–12526.
- 39 N. Selvakumaran, A. Pratheepkumar, S. W. Ng, E. R. T. Tiekink and R. Karvembu, *Inorg. Chim. Acta*, 2013, **404**, 82–87.